Catalyst Kinetics and Stability in Homogeneous Alcohol Acceptorless Dehydrogenation

Martin Nielsen

Additional information is available at the end of the chapter

Abstract

The anthropogenic climate changes caused by meeting the energy demands of society by use of fossil fuels render the development of benign alternatives imperative. Probably, the most promising alternative is generating energy by means of power units driven by, e.g., solar, wind, water, etc., and then storing the energy that is not immediately used in battery type devices. Such a device might consist of hydrogen chemically stored as alcohol(s). The advantage of this method is that it allows gaseous hydrogen to be stored much more efficiently when liquefied as an alcohol. Moreover, as will be shown in this review, it is possible to release the hydrogen under mild conditions when employing homogeneous catalysis. This review considers the kinetic aspects of homogeneously catalysed acceptorless alcohol dehydrogenation reactions. For clarity, the sections are divided according to alcohol substrate, and each metal are described and discussed in subsections. Moreover, the kinetic information in the homogeneously catalysed AAD is traditionally provided simply as the turnover frequency, and more in-depth studies on the actual kinetic parameters are to date still largely elusive.

Keywords: homogeneous catalysis, acceptorless dehydrogenation, alcohols, catalyst kinetics, catalyst stability

1. Introduction

Acceptorless alcohol dehydrogenation (AAD) is the extrusion of H_2 from alcohols resulting in H_2 and carbonyl products. The latter includes, e.g., aldehydes, ketones, esters, amides, carboxylic acids, and CO_2. Conducting AAD by means of homogeneous catalysis is a promising approach towards a viable applicable energy carrier technology. For example, the vision with "Methanol economy" [1] is that H_2 produced by renewable energy sources is stored and transported in MeOH. The reasons for doing so are that H_2 is unfeasible to transport and that

INTECH
open science | open minds

renewables are intermittent energy sources, which is unfit with the continuous energy need from society. Another example is the direct use bioalcohols as H_2 sources. It can be envisioned that the H_2 can be stored directly in the renewables by using, e.g., bioethanol or glycerol as the resource materials.

Besides the energy application, AAD has demonstrated its usefulness in a plethora of preparative systems. This type of chemistry focuses mainly on the transformation of organic functional groups and will as such not be covered in this review.

Charman studied the fundamental principles of AAD with isopropanol as a model substrate and $[RhCl_6]^{3-}$ as a catalyst in the 1960s [2], and Robinson made further advances in the 1970s [3, 4]. As such, the field of AAD has been active for more than 5 decades. Nevertheless, it can be argued that the area is still immature and much fundamental research is still imperative to take the technology towards methods feasible for commercial application. This review aims to contribute to that end by shedding light on the kinetics and stabilities of various AAD systems mainly developed in the last approximately 10 years. For brevity, focus will be on contributions that provide both catalyst activity and longevity investigations on reactions using isopropanol, ethanol, or methanol.

2. Secondary alcohols

Secondary alcohols are notoriously easier to dehydrogenate than primary alcohols for several reasons. The resulting ketone from dehydrogenating a secondary alcohol is more stable than the corresponding aldehyde, both from a thermodynamic and kinetic perspective. In addition, the aldehyde may easily react further reaching more oxidised functional groups, such as ester, carboxylic acid, or amide depending on the reaction conditions.

2.1. Isopropanol

In 1967, Charman reported that a turnover frequency (TOF) of approximately 14 h^{-1} can be achieved by employing a mixture of 7.6×10^{-3} M (580 ppm) $RuCl_3$, 9.4×10^{-2} M LiCl and 5.5×10^{-2} M HCl in refluxing isopropanol [2]. A decade later, Robinson reported that a combination of 4.45×10^{-2} M (3400 ppm) of $[Ru(OCOCF_3)_2(CO)(PPh_3)_2]$ and 12 equivalent trifluoroacetic acid in refluxing isopropanol led to an initial TOF of approximately 13 h^{-1} [3, 4]. After an additional 10 more years, Cole-Hamilton demonstrated that a TOF of 330 h^{-1} could be reached by using 1.96×10^{-4} M (15 ppm) $RuH_2(N_2)(PPh_3)_3$ and 1 M NaOH at 150°C [5]. The Charman and Robinson systems employ acidic environments, whereas the Cole-Hamilton system is alkaline. However, a direct comparison between the systems and the effect of the additive is hampered by the large reaction temperature and catalyst loading differences, where Cole-Hamilton uses a reaction temperature highly elevated and considerably less concentrated catalyst compared to the others.

In general, the mechanisms were believed to involve an inner-sphere β-hydride elimination of the alcohol followed by proton-assisted H_2 extrusion from the organometallic catalytic intermediate. The proton source would be the acid when present (Charman and Robinson systems); otherwise, the alcohol itself served as the proton donor, which concurrently formed

an activated alcoholate more prone for β-hydride elimination. Hence, a bimolecular transition state involving the transient catalyst intermediate and either the acid or alcohol is evoked.

Robinson observed that the catalytic efficacy was heavily depending on the stoichiometry of the trifluoroacetic acid, corroborating its involvement in the rate-determining catalytic step(s). **Figure 1** illustrates the main elemental steps of the proposed catalytic cycle. Commencing with complex **A**, isopropanol coordination leads to **B**, which is then ready for extrusion of trifluoroacetic acid. Upon this extrusion, the β-hydride elimination leads to an acetone coordinated complex **C**, and complex **D** is then formed by extruding the acetone molecule. Hydrogen formation from complex **D** occurs by trifluoroacetic acid mediated protonation of the hydride in **D**, which then also regenerates complex **A** and thereby closes the catalytic cycle.
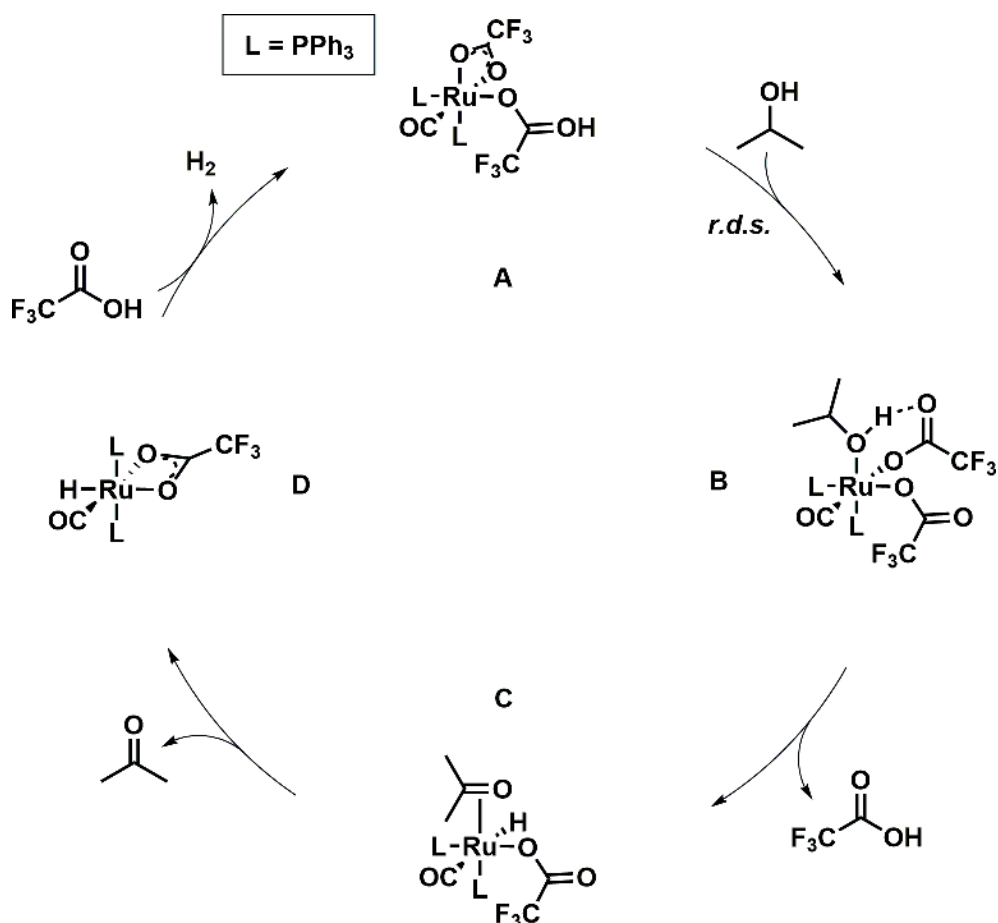

Figure 1. Main proposed elemental catalytic steps of the Robinson isopropanol AAD system. Best result: TOF = 13 h^{-1}.

The steps **B** to **C** and **D** to **A** both involve trifluoroacetic acid as a crucial player. In the former, the acid is extruded, whereas in the latter, it is used as hydride protonation agent and for the re-coordination of trifluoroacetate. Hence, the two steps prefer a low and high acid concentration, respectively, explaining an optimal situation of the 12 equivalents to the Ru complex with respect to obtaining the highest TOF. Moreover, at high acid concentration, the alcohol coordination step (**A** to **B**) appeared to be the rate-determining step.

Contrary, the Cole-Hamilton approach utilises an alkaline-based mechanism, as outlined in **Figure 2**. Commencing with complex **A**, that is, the result of N_2 dissociation from $RuH_2(N_2)$ $(PPh_3)_3$, isopropylate coordinates leading to anionic intermediate **B**. A β-hydride elimination and acetone dissociation then form the trihydride complex **C**, which is sufficiently basic to deprotonate isopropanol to yield the dihydride dihydrogen species **D** and regenerate isopropylate. Finally, loss of H_2 closes the catalytic cycle. This step was found to be the rate-determining, which was corroborated by an incremental effect on the TOF by applying a 500 W tungsten halogen light source.

In 2005 [6] and 2007 [7], Beller developed isopropanol AAD systems based on mixtures of a ligand and either a Ru(II) or Ru(III) precursor in refluxing isopropanol containing 0.8 M NaOiPr. Thus, using two equivalents of 2-di-*t*butyl-phosphinyl-1-phenyl-1*H*-pyrrole to 315 ppm of $RuCl_3$ resulted in a TOF of 155 h^{-1} after 2 h (TOF$_{2h}$) [6], and five equivalents of tetramethylethylenediamine (TMEDA) to 2.0 ppm of [RuCl$_2$(p-cymene)]$_2$ gave a TOF$_{2h}$ of 519 h^{-1} [7].

The authors note a clear catalyst activity dependence on the loading of [RuCl$_2$(p-cymene)]$_2$ [7]. Hence, with 8 and 40 ppm of [RuCl$_2$(p-cymene)]$_2$ with 0.5 equivalents TMEDA, TOF$_{2h}$'s of 309 and 161 h^{-1}, respectively, are observed. Therefore, similar activities are obtained when employing 315 ppm (RuCl$_3$/two 2-di-*t*butyl-phosphinyl-1-phenyl-1*H*-pyrrole) and 40 ppm
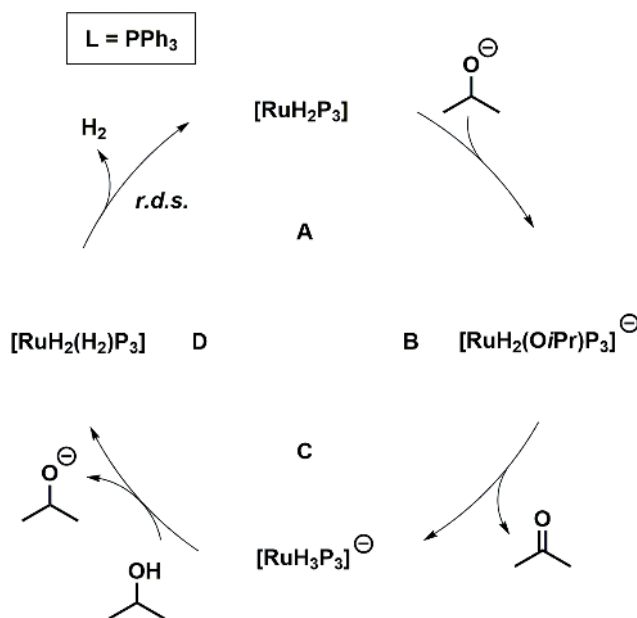

Figure 2. Proposed mechanism for the Cole-Hamilton isopropanol AAD system. Best result: TOF = 330 h^{-1}.

([RuCl$_2$(*p*-cymene)]$_2$/0.5 TMEDA) (155 vs. 161 h^{-1}, respectively). The authors did not carry out activity studies using similar Ru loadings, and it is therefore not possible to make a direct comparison between the two systems. The trend of the catalyst loading effect in the 2007 paper does suggest, nevertheless, that this system would in fact be less active than the 2005 system when using similar Ru loadings.

The fact that lowering the catalyst loading of [RuCl$_2$(*p*-cymene)]$_2$/TMEDA leads to a more active catalytic system might indicate that an associative/dissociative process is involved (*vide infra*) [10]. However, this was not discussed in the paper [7].

Moreover, the 2.0 ppm ([RuCl$_2$(*p*-cymene)]$_2$/five TMEDA) system was allowed to run for 11 days, at which point it was still active and it had reached a turnover number (TON) of 17,215, corresponding to an overall TOF of 64 h^{-1} [7]. No mechanism was proposed.

In 2011, Beller reported on a bis-isopropyl phosphorous substituted phosphorous-nitrogen-phosphorous (PNP^{iPr}, see **Figure 3**) pincer ruthenium catalyst [RuH$_2$(PNP^{iPr})CO] [8, 9] that, when formed *in situ* from mixing 1:1 [RuH$_2$(PPh$_3$)$_3$CO] and PNP^{iPr} ligand, dehydrogenates isopropanol *via* a proposed outer-sphere β-hydride elimination contrary to the until then suggested inner-sphere approaches [9]. The PNP ligand holds an amine unit which deprotonates under somewhat mild conditions leading to an amide-ruthenium bond. Hence, the ligand plays a cooperative role during the catalytic cycle. This setup allowed for conducting the AAD under neutral conditions without using any additives.

Moreover, this led to a drastic increase in TOF with an observed TOF$_{max}$ of 14,145 h^{-1} when employing a 4.0 ppm loading of the catalyst in refluxing isopropanol. This corresponds to a more than 25-fold increase in catalyst turnover frequency compared to the previous state-of-the-art [7]. Interestingly, adding merely 1.3 equivalent of Na*i*OPr in fact led to an approximately 10% decrease in TOF. Moreover, screening results suggested that the CO was vital for obtaining any AAD activity and that exchanging one of the hydrides with a chloride rendered the addition of 1.3 equivalent of Na*i*OPr necessary. The latter suggests that the role of the base in this case is to eliminate off the chloride, thus generating complex **A** in **Figure 3**.
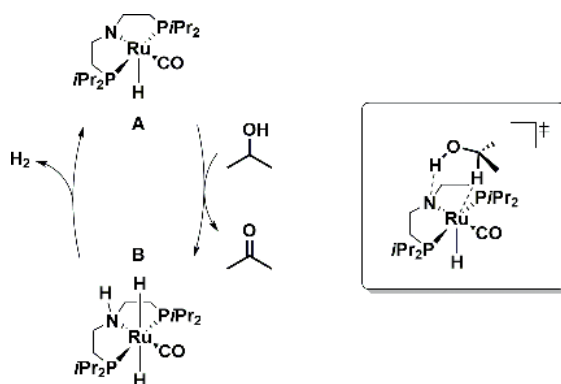

Figure 3. Proposed mechanism for the Beller isopropanol AAD system. Best results: TOF = 14,145 h^{-1}. TON > 40,000. Stable for more than 12 h.

When increasing the catalyst loading eight times from 4.0 to 32 ppm, a fourfold decrease in TOF_{2h} was observed (8342–2048 h^{-1}). This was not addressed further, but it might be speculated whether a detrimental association of two catalyst molecules is more likely at a higher concentration (*vide infra* for more discussions on this topic) [10].

A TON of more than 40,000 was achieved after merely 12 h, compared to the 17,215 after 11 days in the previous AAD report by Beller [7]. Notably, the system was noted to be still highly active after the 12 h. In this regard, it might be speculated whether the chelating pincer ligand renders the catalytic complex particularly robust and thus enables a prolonged lifetime of the system.

Figure 3 shows the proposed mechanism. Because no additives or protonation/deprotonation steps are involved during the catalytic cycle, the entire cycle is composed of two elemental steps, β-hydride elimination of the isopropanol and dehydrogenation of the catalyst. This fact might contribute to the markedly enhanced catalytic activity.

As mentioned, the two steps involve the outer-sphere β-hydride elimination of isopropanol by complex **A** leading to acetone and complex **B** followed by H_2 formation and extrusion, thus regenerating **A**. According to the suggested mechanism, the ligand nitrogen atom plays a fundamental role in both steps. Hence, during the first step, the amide functionality coordinates to the alcohol proton thereby enhancing the carbon-based hydride abstraction. Similarly, the amine serves as proton transferring source to the alkaline hydride leading to the H_2 production.

Overall, the kinetics and longevity of the catalytic systems for isopropanol AAD seem to be highly influenced by the catalytic mechanism and of the necessity of an additive involved in it. Moreover, it is clearly feasible to effectively both dehydrogenate isopropanol and subsequently extrude H_2 without any additive-mediated catalyst activation. Thus, devising a system that employs as simple a mechanism as possible and that are in the absence of catalytic sinks might be important facets to strive for designing new AAD catalysts in the future.

It remains to be disclosed whether an inner- or outer-sphere β-hydride elimination is the key to reaching the superior catalyst activity demonstrated by Beller. Thus, more investigations on this topic would be interesting.

3. Primary alcohols

3.1. Ethanol

In 1987, Cole-Hamilton demonstrated that EtOH can be dehydrogenated with a TOF of 96 h^{-1} by 1×10^{-3} M (61 ppm) [Rh(bipy)$_2$]Cl in EtOH containing 5% v/v and 1.0 M NaOH at 120°C [11]. The same group improved on this in 1988 [5] and 1989 [12] with a TOF of 210 h^{-1} by use of 3.48×10^{-4} M (20 ppm) $RuH_2(N_2)(PPh_3)_3$, 1 M NaOH, and an intense light source at 150°C. Mechanistic considerations similar to those described for isopropanol (**Figure 2**) were discussed.

In 2012, Beller demonstrated that the same catalytic system that showed superiority with respect to isopropanol AAD (**Figure 3**) also provide interesting results with ethanol [9] Hence, a TOF_{2h} of 1483 h^{-1} could be achieved when using 3.1 ppm 1:1 [RuH$_2$(PPh$_3$)$_3$CO] and PNP^{iPr} ligand in refluxing neutral ethanol. Both acetaldehyde and ethyl acetate were observed as

products in substantial amounts. The former product might explain the decrease in activity (TOF_{6h} = 690 h^{-1}) due to a reversible dehydrogenation/hydrogenation process. Moreover, a similar mechanistic rationale as depicted in **Figure 3** was provided.

A constant catalyst activity towards full conversion of ethanol to ethyl acetate can be achieved by adding a minute amount of Na*i*OPr [13] Hence, when using 50 ppm of the commercially available Ru-MACHO ([RuHCl(PNP^Ph)CO]) in refluxing ethanol for 46 h in the presence of 0.6 mol% NaOEt, a 77% yield of ethyl acetate (TON = 15,400) was obtained. This could be increased slightly to 81% when using 500 ppm catalyst loading and 1.3 mol% NaOEt. Interestingly, a yield of 70% was obtained when conducting the reaction at merely 70°C.

Studies into the effect of additive composition were undertaken. This provided two main results. First, NaOEt was superior to KOEt, NaOH, K_2CO_3 and Cs_2CO_3. Second, an optimal NaOEt loading with respect to maximising the TOF was observed.

Moreover, the 1:1 [RuH$_2$(PPh$_3$)$_3$CO]/PNP^iPr ligand combination showed similar activity to Ru-MACHO with TOF's of the former of 1107 and the latter of 1134 h^{-1} when employing 25 ppm catalyst loading and 1.3 mol% NaOEt.

Notably, with Ru-MACHO, the conversion rate is practically constant until 90% of the ethanol is used up, at which point the NaOEt is precipitating out of the reaction. This resulted in a TOF_{2h} of 934 h^{-1} and TOF_{10h} of 730 h^{-1} when using 50 ppm catalyst loading. Hence, it was concluded that the reverse hydrogenation process of ethyl acetate was occurring at a negligible level.

Again, a similar mechanism to the one depicted in **Figure 3** was suggested. However, as shown in **Figure 4**, this now involved the dehydrogenation of two different species. Hence, initially ethanol is dehydrogenated into acetaldehyde, which then reacts with either an ethanol or an ethoxide to generate a hemiacetal or anionic hemiacetal intermediate. This compound then undergoes the second dehydrogenation step, leading to another H_2 molecule and the ethyl acetate product.
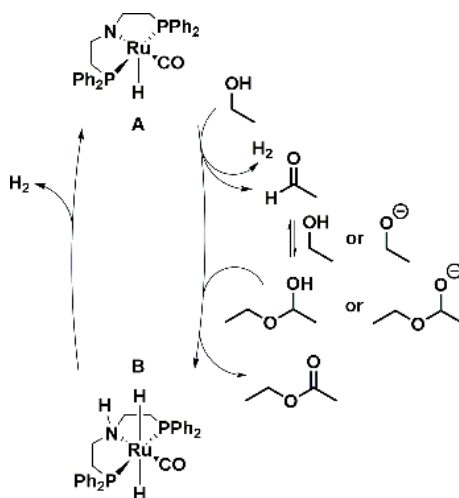

Figure 4. Proposed mechanism for the Beller ethanol AAD to ethyl acetate system. Best result: TOF = 1137 h^{-1}. TON = 15,400. Yield = 81%. Stable for more than 46 h.

In 2012, Gusev reported that the NNP ruthenium species **2**, depicted in **Figure 5**, is superior to Ru-MACHO [10] The Gusev setup employs a slightly modified setup compared to the Beller setup (i.e., less NaOEt, and shorter reaction times than in the Beller setup), and a direct comparison of the results is therefore not feasible. Nevertheless, Gusev also tested the Ru-MACHO catalyst with his system, allowing for direct comparisons of the catalysts.

Thus, in the Gusev setup, 50 ppm Ru-MACHO in refluxing ethanol containing 1 mol% NaOEt led to 42% conversion after 40 h. An impressive 85% conversion was observed under the same conditions with complex **2**, clearly demonstrating the superiority of this catalyst. Moreover, a TOF_{24h} was 567 h^{-1}. Furthermore, 50 ppm **2** was able to reach 83% conversion of simple anhydrous commercial ethanol to ethyl acetate in the presence of air. Hence, air or water seems to have no detrimental influence on catalyst activity. In this regard, it should be noted that all other the reactions performed by Gusev and Beller are done under rigorously inert conditions.

A rather extensive catalyst screening was performed with ruthenium and osmium as transition metals, which **Figure 5** shows a selection of. A quick survey reveals that Ru-MACHO, **1**, and **3** perform similar levels despite **3** being significantly different than the two former complexes. Moreover, changing the *P*-substituents from phenyl to isopropyl seems to have no influence of the conversion, which is in line with the Beller findings. On the other hand, exchanging the CO in **3** to a PPh$_3$ in **2** drastically increases the conversion, which is contrary to the Beller observations that concluded the CO to be crucial for achieving activity. Moreover, when employing the trihydride osmium(IV) species **4**, practically no conversion is observed.

The influence of the metal can be directly compared in complexes **1** and **5** and in **3** and **6**. Thus, the PNP ruthenium-based **1** shows a slightly superior activity than the osmium-based congener **5** (47% conversion versus 35% after 24 h), whereas the PNN ruthenium-based **3** is noticeably more active than the osmium-based **6** (42 versus 13%). Thus, the PNN ligand seems
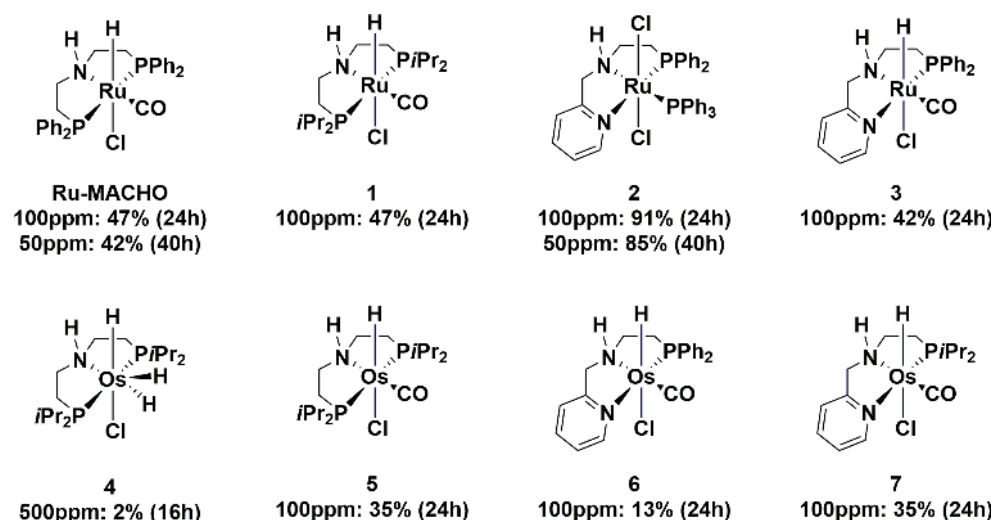

Ru-MACHO
100ppm: 47% (24h)
50ppm: 42% (40h)

1
100ppm: 47% (24h)

2
100ppm: 91% (24h)
50ppm: 85% (40h)

3
100ppm: 42% (24h)

4
500ppm: 2% (16h)

5
100ppm: 35% (24h)

6
100ppm: 13% (24h)

7
100ppm: 35% (24h)

Figure 5. Selection of the complexes tested for ethanol AAD to ethyl acetate by Gusev. Best result: 85% conversion with 50 ppm after 40 h.

considerably more susceptible to the choice of metal than the PNP ligand, suggesting that two, or more, different mechanisms are operating.

Finally, the low conversion obtained with complex **6** could be improved on by simply exchanging the *P*-phenyl substituents with isopropyl (13% with **6** versus 35% with **7**).

A mechanism akin to the depiction in **Figure 4** was suggested. Furthermore, H_2 extrusion from the hydrogenated form of **2** was proposed. Moreover, as Beller observed for isopropanol AAD [9], it was noted that decreasing the catalyst loading had a beneficial effect on the TOF. As such, the TOF_{24h} was 375 h^{-1} with 100 ppm and 567 h^{-1} with 50 ppm. It was in this respect suggested that an associative/dissociative process was involved. Varying the loading of the osmium dimer in **Figure 6** further corroborates such a process. Thus, when reducing the catalyst loading from 500 to 100 ppm, the TOF likewise increased approximately five-fold (56–275 h^{-1}). This has the striking consequence that after 24-h reaction time, the 100 ppm loaded mixture afford 66% conversion, whereas the 500 ppm only provide 45%.

In 2014, Beller demonstrated that bioethanol can be effectively converted to acetate by AAD [14]. The complex [RuHCl(PNP^{iPr})CO] provide the best catalyst turnover, and a TOF_{1h} of 1770 h^{-1} is observed when employing 25 ppm catalyst loading in refluxing wet bioethanol containing 8 M NaOH. This result is similar to that found when employing dry ethanol [9] (1770 versus 1483 h^{-1}) albeit at severely harsher conditions. The highly alkaline media was necessary to maintain the product in a deprotonated state, presumably to avoid catalyst deactivation by coordination of acetic acid to the catalyst. Moreover, a 70% yield was obtained within 20 h when using a 1:1 EtOH/H_2O mixture. In addition, a long-term reaction with 10 ppm catalyst loading reached a TON 80,000 after 98 h.

Overall, the results with ethanol clearly demonstrate that primary alcohols are notoriously more difficult to achieve high TOF with than with secondary congeners. Thus, when comparing state-of-the-art turnover frequencies of ethanol AAD (1770 h^{-1}) [14] with that for isopropanol (14,145 h^{-1}) [9], there is an order of magnitude difference in favour of the latter.

Moreover, there is still a lack of studies into the mechanism of the various discrete catalytic steps. Shedding light on these would provide a deeper insight into the kinetic features and parameters of primary alcohol AAD by homogeneous catalysis.

3.2. Methanol

In 1987, Cole-Hamilton demonstrated that MeOH can be dehydrogenated with a TOF of 7 h^{-1} by 1×10^{-3} M (43 ppm) [Rh(bipy)$_2$]Cl in MeOH containing 5% (v/v) H_2O and with 1.0 M NaOH at 120°C [11]. This was the year later improved to 37.3 h^{-1} by the same group by use of 1–5 ×

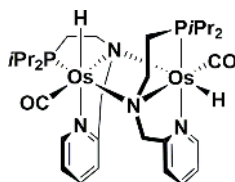**Figure 6.** PNN osmium dimer by Gusev. 500 ppm: 45% conversion (24 h), 100 ppm: 66% conversion (24 h).

10^{-4} M (4–20 ppm) $RuH_2(N_2)(PPh_3)_3$, 1 M NaOH, and an intense light source at 150°C [5]. A mechanism as depicted in **Figure 2** was proposed.

In 2013, Beller disclosed a procedure for homogeneously catalysed aqueous-phase reforming type conversion of $MeOH/H_2O$ mixtures to $3H_2$ and CO_2 (or other C_1 residuals, such as carbonate, see **Figure 7**) [15]. Using 1.6 ppm of [RuHCl(PNP^{iPr})CO] in MeOH with 8.0 M KOH at 95.0°C afforded a TOF_{1h} of 4719 h^{-1}. Furthermore, using 19 ppm of [RuHCl(PNP^{Ph})CO] with respect to MeOH in a 9:1 (v/v) $MeOH/H_2O$ mixture afforded a TOF_{1h} of 63 h^{-1} at 65°C. As a note, the TOF was counted in such way that a complete reaction of $MeOH/H_2O$ mixtures to CO_2 and $3H_2$ sums as three turnovers. This was done because all three reactions depicted in **Figure 7** occurs simultaneously, rendering any quantitative kinetic discrimination between them unpractical.

The system turned out to be very robust, with a TON over 350,000 and reaction time exceeding 23 days when using 1 ppm catalyst loading with respect to MeOH of [RuHCl(PNP^{iPr})CO] in a refluxing 9:1 (v/v) $MeOH/H_2O$ solution containing 8.0 M KOH. Moreover, after the 23 days a 27% yield of full MeOH reforming was achieved (based on H_2 evolution and yield based on H_2O as the limiting factor. The yield is 12% with respect to MeOH). When using 150 ppm, a CO_2-based yield of 43% was reached within 24 h (yield based on H_2O as the limiting factor. The yield is 19% with respect to MeOH).

It was also demonstrated that a continuous production of a 3:1 H_2/CO_2 gas mixture, and hence full MeOH reforming, can be achieved by employing 250 ppm catalyst loading with respect to MeOH of the [RuHCl(PNP^{Ph})CO] in a refluxing 4:1 (v/v) $MeOH/H_2O$ solution containing 0.1 M NaOH. After an initiation time of approximately 5–6 h, the expected 3:1 ratio of H_2 and CO_2 was observed in the gas mixture. In addition, the pH dropped from 13 to approximately 10 during the first 4 h. It was suggested that during this initiation time, the hydroxide was reacting with formic acid and CO_2 leading to an eventual equilibrium between hydroxide/(bi) carbonate/formate as the C_1 residuals.

The catalyst activity was depending on a range of factors. Besides the reaction temperature the pH, base additive, and catalyst loading all influenced the activity. As such, a higher pH and lower catalyst loading promoted an increased turnover frequency. The latter is in agreement
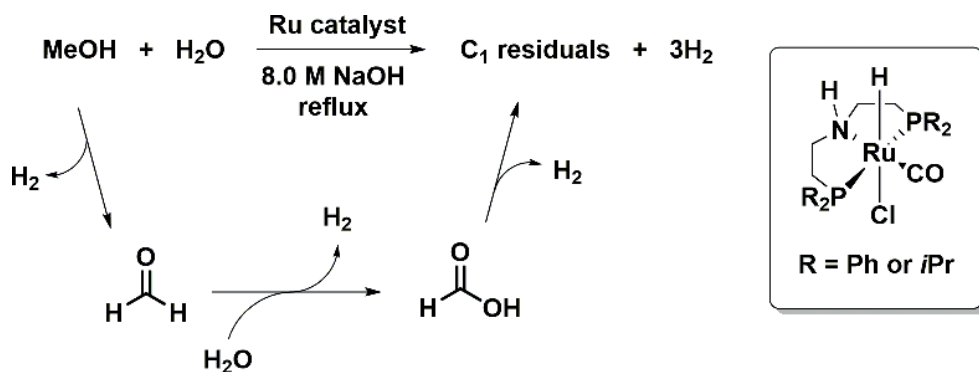

Figure 7. Aqueous MeOH AAD to $3H_2$ and C_1 residuals by Beller. Best results: TOF = 4719 h^{-1}. TON > 350,000. Yield = 43%. Stable for more than 23 days.

with previous observations by, e.g., Beller [9] and Gusev [10]. Moreover, the requirement of a high pH to induce high catalyst activity might reflect the tendency of the catalyst to reside in a range of resting states, particularly with a coordinating formic acid. In order to re-activate the catalyst, a base can eliminate off, e.g., the formic acid from the resting catalyst.

Catalyst TOF dependency on pH is likely also a major reason for the influence of base additive. However, Bernskoetter, Hazari, and Holthausen demonstrates in a later publication that the cationic counter ion might very well play a crucial role as well (*vide infra*) [16]. Even though they employ modified reaction conditions, the same effect of the cation might also be in play in the Beller setup.

An in-depth study revealed several aspects of the mechanism(s) [17]. An Arrhenius plot revealed the temperature-activity dependency, and with [RuHCl(PNP^{iPr})CO] an activation energy of E_a = 82.4 kJ/mol and A = 1.2 × 10^6 mol/s were found. Furthermore, a kinetic isotope effect (KIE) of 7.07 was observed, strongly suggesting proton involvement in the rate-determining step. However, because three reactions are concomitantly taking place, any further conclusions on the mechanism are difficult. Moreover, at certain catalyst loadings the gas evolution initially follows pseudo zero kinetics. The same incremental effect on TOF upon decreasing the catalyst loading was observed as well, providing a reaction order with respect to the catalyst of less than 1. Finally, computational studies were employed to shed further light on the mechanism(s).

This led to a revised suggested mechanism. Overall, the ruthenium-amido functionality still plays a key role, but an inner-sphere mechanism for the β-hydride elimination involving, e.g., a methoxide for the MeOH dehydrogenation step was discussed and proposed. In addition, the dehydrogenation step is assisted by a MeOH molecule, akin to previously described by Schneider [18]. Hence, in the latter step, a transient protonation of one of the hydrides may be involved.

Interestingly, the *N*-methylated congener to the isopropyl *P*-substituted catalyst was tested as well. Considering the key role of the amine/amido unit of the so far proposed mechanisms, a drastic drop in TOF was expected. However, surprisingly a mere drop of 2.4 times in catalyst activity was observed. However, a KIE of 1.76 suggests a change in mechanism. Furthermore, a bell-shaped activity dependency on KOH concentration with a maximum activity at 4.0 M KOH was observed. In fact, at this base concentration, the *N*-methylated catalyst is almost twice as active than the original one at 60°C (approximately 100 versus approximately 50 h^{-1}) and approximately 50% more active at 90°C (approximately 200 versus approximately 125 h^{-1}).

These results all clearly point towards a change in mechanism upon methylating the ligand nitrogen atom. Moreover, computational studies suggested that a higher stability towards hydride protonation was responsible for the bell-shaped activity-base concentration behaviour.

Beller later showed that by mixing Ru-MACHO-BH (chloride of Ru-MACHO exchange with a borohydride) with [Ru(H)$_2$(dppe)$_2$], MeOH reforming can be achieved under neutral conditions [19]. Thus, mixing 22.5 ppm with respect to MeOH of each of the catalysts in a 9:1:4 (v/v) mixture of MeOH/H$_2$O/triglyme at 93.5°C applied temperature afforded a TOF$_{1h}$ of 87 h^{-1}. A long-term experiment afforded a 26% yield to H$_2$O, corresponding to a TON > 4200.

Even though this value is considerably lower than for the system containing base, it still proofs the principle of base-free MeOH reforming. Interestingly, the combination of the two catalysts provided a system significantly more active than the sum of the two catalysts individual performance.

In 2013, Grützmacher devised another catalytic system for methanol reforming by homogeneously ruthenium catalysed AAD under neutral conditions [20]. Conducting the MeOH reforming using 500 ppm of $[K(dme)_2][Ru(H)(trop_2dad)]$ (**A** in **Figure 8**) in refluxing THF containing a 1:1.3 mixture of $MeOH/H_2O$ (90°C applied temperature) afforded 90% conversion after 10 hours, corresponding to an overall TOF of 54 h^{-1} and TON of 540. Moreover, the yield was 84% yield.

The proposed mechanism using $[K(dme)_2][Ru(H)(trop_2dad)]$ is markedly different from that using $[RuHCl(PNP^{iPr})CO]$ as catalyst. As shown in **Figure 8**, the ruthenium is redox active during the catalytic cycle. Hence, commencing with complex **A** ($[Ru(H)(trop_2dad)]^-$) containing a Ru^{II} center, a water assisted hydride protonation and subsequent dehydrogenation to species **B** with unspecified oxidation state is occurring. MeOH then adds to the Ru-N bond affording complex **C**, which has a Ru^{II} center. A β-hydride elimination then leads to the extrusion of formaldehyde, which reacts with water to give methanediol. Furthermore, the metal center is reduced to Ru^0 and the singly protonated 1,2-enediamide moiety in **C** becomes further protonated to yield the amino imine complex **D**. The methanediol is then dehydrogenated by **D** to yield formic acid and the imine moiety in **D** is reduced to afford diamine complex **E**, which upon de-coordination of the formic acid leads to species **F**. Hence, at this stage, complex **B** has taken up two equivalents of H_2. Finally, a base-assisted dehydrogenation of the ligand framework and consequently oxidation of the ruthenium converts **F** back to **A**, thereby closing the catalytic cycle.

Computational studies indicate that the conversion of methanediol to formic is faster than the conversion of MeOH to methanediol, explaining the absence of formaldehyde during the reaction. Moreover, it was demonstrated that complex **A** efficiently catalyses the dehydrogenation of formic acid to H_2 and CO_2. Thus, employing a 100 ppm catalyst loading in a 1 M formic acid solution in dioxane at 90°C provided an initial TOF of 24,000 h^{-1}.

In 2014, Milstein also disclosed a catalytic system for MeOH reforming by AAD [21]. A catalyst loading of 250 ppm (with respect to MeOH) of the PNN ruthenium complex shown in **Figure 9** in a 5.55:1 mixture of $MeOH/H_2O$ in toluene at 100–105°C (115°C applied temperature) in the presence of two equivalents of KOH with respect to MeOH was employed. This led to a H_2-based yield of 77% after 9 days. Interestingly, the organic layer of the reaction could be isolated and reused for another round of MeOH reforming. Doing so twice led to an overall TON of approximately 29,000 with a yield after the third round of 80%, again after 9 days. Hence, the system seems feasible for reusing, which is an important factor for developing applicable MeOH reforming systems.

The decomposition of formic acid to H_2 and CO_2 was also studied. When employing 900 ppm of the catalyst, 1.2 equivalents of KO*t*Bu with respect to catalyst, and pure formic acid in a 1:1 (v/v) THF/H_2O mixture a mere 25% conversion was observed after 24 h. This was improved to >99% upon exchanging the KO*t*Bu with two equivalents of KOH. Interestingly, when no H_2O was present, a reaction containing two equivalents of Et_3N as base leads to 98% conversion after 24 h at room temperature. It was thus concluded that formic acid decomposition is markedly more facile than its formation from methanol. Hence, the first two steps of the MeOH reforming were suggested to be rate-determining. Moreover, mechanistic studies suggest that one of the ligand methylene hydrogens takes part of the catalytic cycle *via* dearomatization of the central pyridine unit, such as Milstein has previously demonstrated with other AAD systems [22].
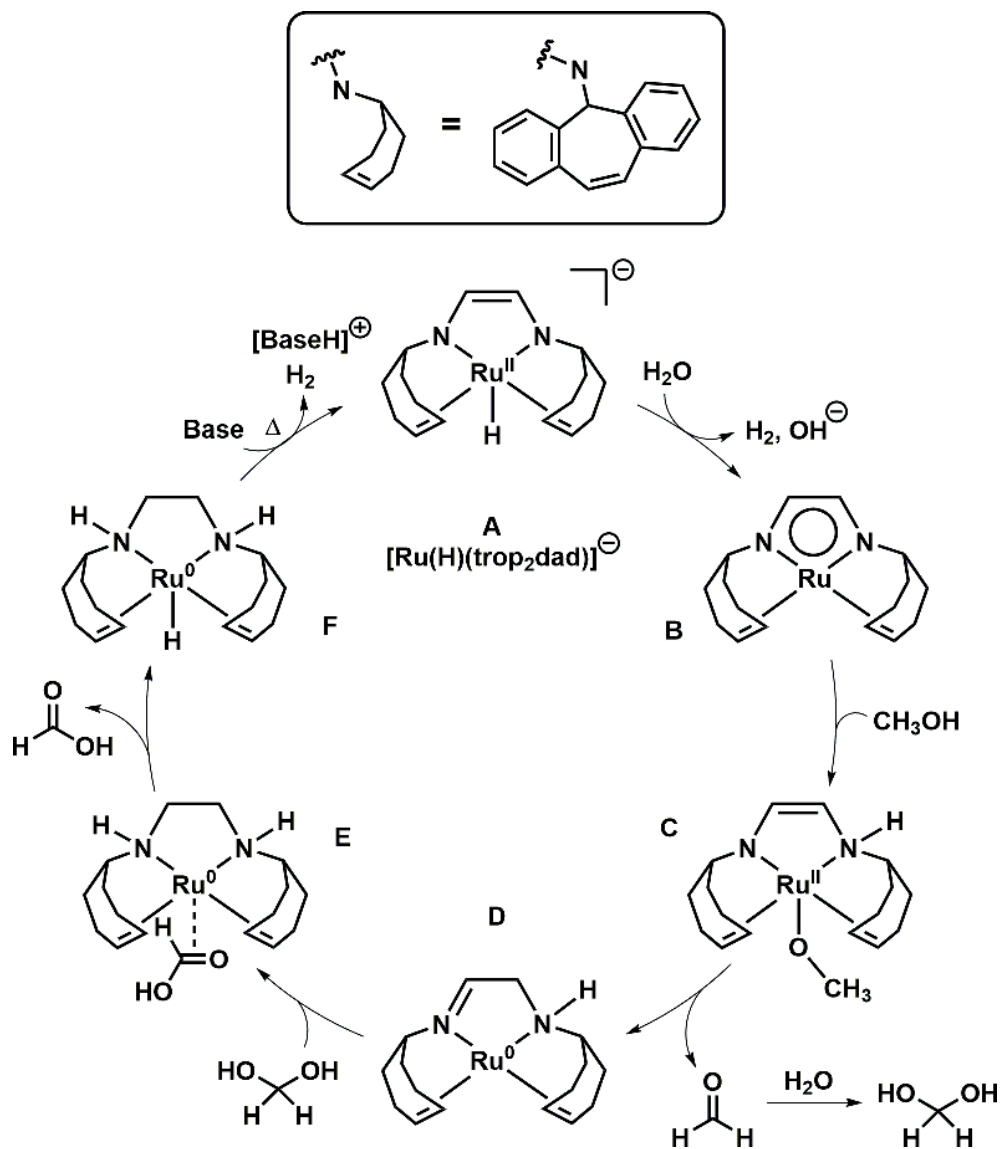
Figure 8. Proposed catalytic cycle for MeOH reforming by Grützmacher using MeOH as substrate. Best results: TOF = 54 h^{-1}. TON = 540 h^{-1}. Conversion = 90%. Yield = 84%.

The Reek group showed in 2016 that [Ru(salbinapht)(CO)(PiPr$_3$)] (**Figure 10**) is also capable of dehydrogenating MeOH [23]. A TOF value of 55 h^{-1} could be reached by a catalyst loading of 24 ppm with respect to MeOH in a 25% dioxane/75% 9:1 (v/v) MeOH/H$_2$O mixture containing 8 M KOH and conducting the reaction at 82°C. Lowering the base concentration to 6 M and
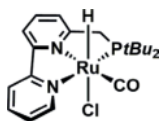
Figure 9. Milstein PNN ruthenium catalyst for MeOH reforming. Best results: TOF = 45 h^{-1}. TON = 29,000. Yield = 82%. Reusable system.
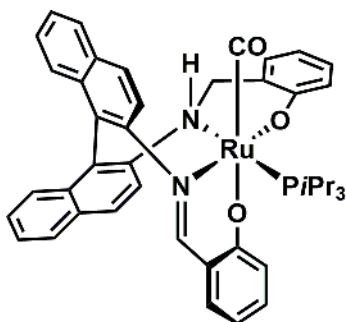

Figure 10. Reek catalyst for MeOH reforming. Best result: TOF = 55 h^{-1}.

4 M afforded TOF's of 37 and 29 h^{-1}, respectively. This was partially explained by the decrease in reaction temperature as a result of the lower base concentration (79°C with the 6 M and 76°C with the 4 M).

It was also revealed that $[Ru(H)_2 (PiPr_3)_2(CO)_2]$ catalyses the reaction with practically the same efficiency (TOF = 50 h^{-1}), leaving some speculations as to whether this is the real catalyst.

Moreover, mechanistic investigations suggest that the CO moiety of [Ru(salbinapht)(CO) (PiPr$_3$)] plays an active role during the catalytic cycle by reacting with hydroxide and thus forming formic acid and H$_2$. This might open for the possibility that a similar mechanism might (partially) take place with the Beller and Milstein systems.

Other metal complexes have also been shown to conduct MeOH reforming by AAD, specifically iron [16, 24], manganese [25], and iridium [26–28]. Several of them are comprised of PNP^{iPr} pincer ligand complexes, such as the iron-based compounds shown in **Figure 11**. Beller initially showed that borohydride coordinated species afforded a TOF$_{2h}$ of 644 h^{-1} when using a 4.5 ppm catalyst loading in a 9:1 (v/v) MeOH/H$_2$O mixture containing 8.0 M KOH and stirring at 91°C [24]. A long-term experiment allowed for a TON$_{46h}$ of 9834.

When comparing this result using the iron-based catalyst with the TOF values obtained when using the ruthenium-based congener, the latter is superior with respect to catalyst activity and longevity. Nevertheless, showcasing the feasibility of conducting MeOH reforming using a non-noble metal catalyst is an important step towards applicability, which these findings therefore represent.

Bernskoetter, Hazari, and Holthausen improved the iron-based MeOH reforming by exchanging the borohydride with a formate, dissolving minute amounts of MeOH and H$_2$O in EtOAc,
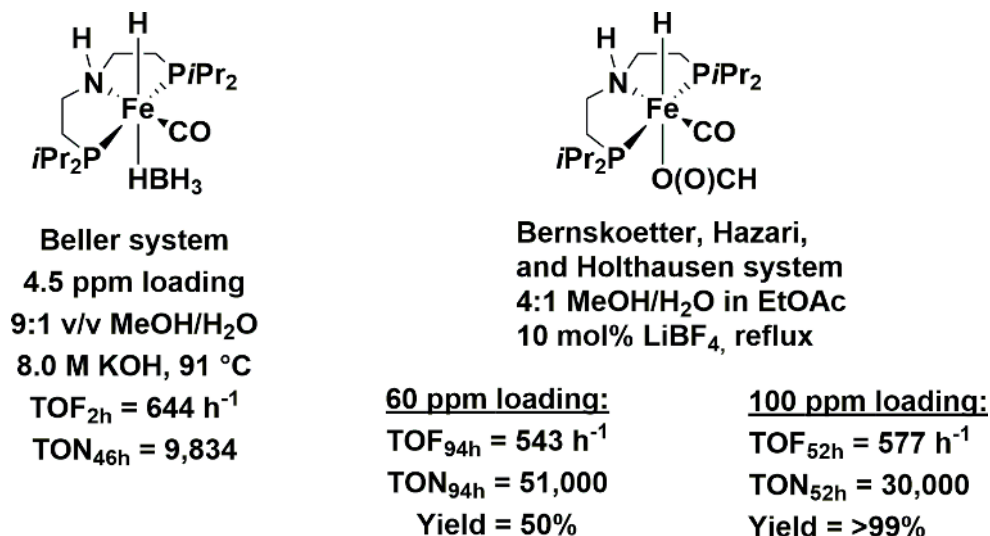
Beller system
4.5 ppm loading
9:1 v/v MeOH/H_2O
8.0 M KOH, 91 °C
$TOF_{2h} = 644$ h^{-1}
$TON_{46h} = 9{,}834$

**Bernskoetter, Hazari,
and Holthausen system**
4:1 MeOH/H_2O in EtOAc
10 mol% LiBF$_4$, reflux

60 ppm loading:
$TOF_{94h} = 543$ h^{-1}
$TON_{94h} = 51{,}000$
Yield = 50%

100 ppm loading:
$TOF_{52h} = 577$ h^{-1}
$TON_{52h} = 30{,}000$
Yield = >99%

Figure 11. MeOH reforming using PNP iron catalysts.

and adding 10 mol% LiBF$_4$ as additive rather than the 8.0 M KOH [16]. By doing so, an impressive TON of 51,000 could be reached after 94 h by using 60 ppm catalyst loading, which corresponds to 50% yield. A >99% yield could be obtained by increasing the catalyst loading to 100 ppm ($TON_{52h} = 30{,}000$).

Based on a number of in-depth studies, including computational insights, the authors suggest that the Lewis acidic Li$^+$ promotes de-coordination of formate and subsequent its dehydrogenation as well, thereby facilitating a faster formic acid decomposition to H_2 and CO_2. Furthermore, they conclude that under neutral conditions, the formation of the methanediol intermediate is mediated by the catalyst as well.

Interestingly, when using dry MeOH in EtOAc, methyl formate can be formed in >99% yield when otherwise similar conditions as the latter mentioned above, thus corresponding to a TON of >19,999.

Recently, Beller used 0.05 mM concentration a [MnBr(PNP^{iPr})(CO)$_2$] complex and additional 10 equivalents of the PNP^{iPr} ligand in a 1:1 (v/v) mixture of 9:1 MeOH/H_2O/triglyme at a applied temperature of 92°C to achieve a TON of more than 20,000 after more than a month. Thus, the system is highly stable albeit with a low turnover frequency. Moreover, the catalytic cycle was suggested to follow the general mechanism depicted in **Figures 3** and **4**.

Fujita and Yamaguchi demonstrated in 2015 that the iridium complex shown in the catalytic cycle in **Figure 12** facilitates MeOH reforming. The best conditions were found to be refluxing a 1:4 MeOH/H_2O mixture containing 0.50 mol% NaOH. Employing a 5000 ppm catalyst loading afforded a 84% yield after 20 h, corresponding to a TON of 5040 and an overall TOF of 252 h^{-1}.

It was furthermore demonstrated that a system containing 1000 ppm is capable of continuously dehydrogenate MeOH. Hence, when a mixture of MeOH, H_2O, and NaOH was continuously
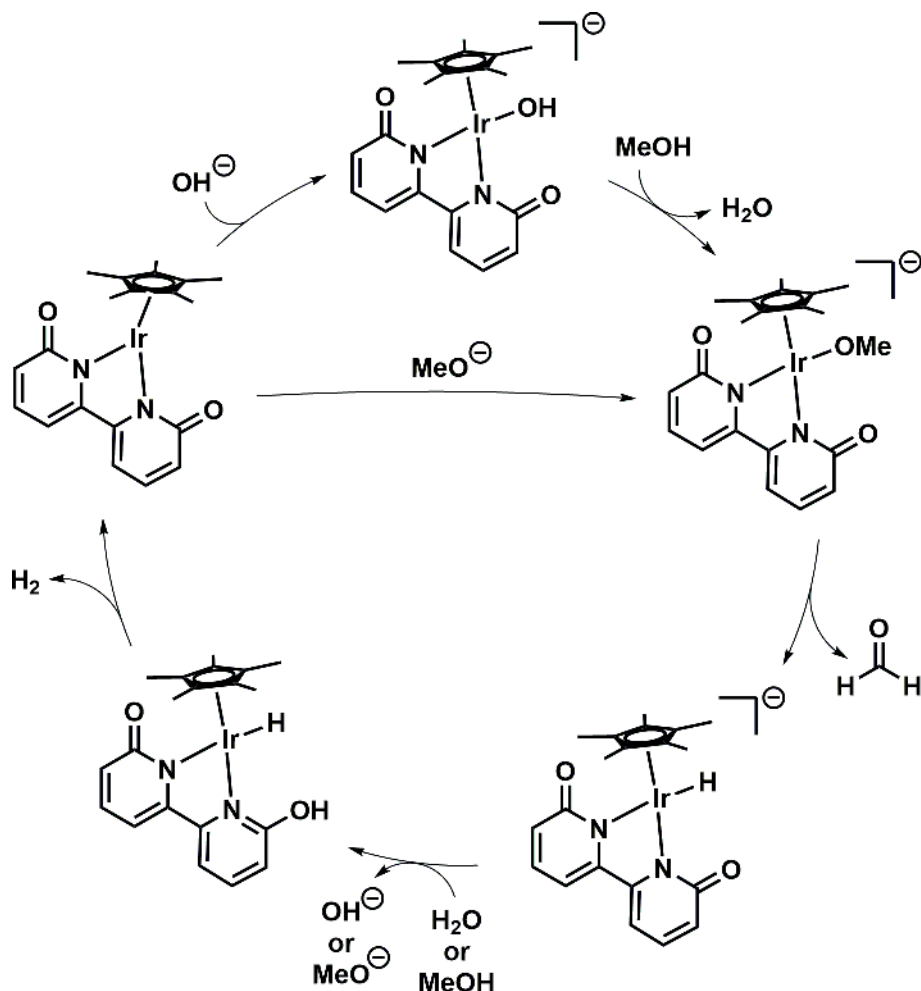
Figure 12. Proposed catalytic cycle for the Yamaguchi system for MeOH reforming.

added dropwise to the solution, a TON of 10,510 was reached after 150 h. This is an important achievement since devising a MeOH reforming system capable of continuously converting MeOH is of application-wise interest.

The catalytic cycle was suggested to follow the mechanism shown in **Figure 12**. Initially, the starting organometallic complex has its hydroxide replaced by a MeOH molecule, which then undergo β-hydride elimination yielding a formaldehyde molecule, that is extruded, and the anionic hydride complex. It is not discussed whether an inner- or outer-sphere β-hydride elimination takes place.

The anionic hydride complex is then prone to protonation at one of the pyridonate moieties, which affords the neutral hydride complex that then undergoes dehydrogenation resulting
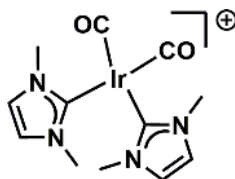
Figure 13. Crabtree catalyst for MeOH dehydrogenation. Best results: TOF_{40h} = 200 h^{-1}. TON_{40h} = 8000.

in the unsaturated tri-coordinated species. Finally, either a hydroxide re-makes the starting catalytic complex, or a methoxide brings the complex straight to the methoxo complex.

The same year, Crabtree demonstrated that the biscarbene iridium complex shown in **Figure 13** is also able to dehydrogenate MeOH [27]. Thus, after 40 h 10 ppm catalyst loading had converted refluxing dry MeOH containing 6.7 M KOH with a TON of 8000, corresponding to an overall TOF of 200 h^{-1}. Moreover, the reaction produced H_2 in a practically linear fashion the first 20 h. Furthermore, the system was found to work in the presence of air, and thus no inert atmosphere was necessary.

Recently, Beller employed a PNP^{iPr} pincer ligated iridium complex for MeOH reforming [28]. At low base concentrations (0.1 M KOH), 19 ppm of $Ir(H)_3(PNP^{iPr})$ in refluxing 9:1 (v/v) MeOH/H_2O (69°C) dehydrogenate MeOH with a TOF_{1h} of 525 h^{-1}. After 16 h, a TON of 1600 was reached after which gas evolution ceased. This could be improved by increasing the base concentration to 8.0 M KOH, in which the system becomes stable for more than 60 h and results in a TON of 1900. Moreover, only a slight drop in catalyst activity was observed during this period.

Interestingly, when increasing the base concentrations, the activity drops. The same is true when lowering the base amount to two equivalents with respect to the catalyst. Hence, a rather small concentration of base is optimal for achieving the best catalytic turnover frequency. Thus, a bell-shaped base-activity curve was observed similar to that for the N-methylated PNP^{iPr} ruthenium-based catalyst (*vide supra*) [18].

Employing $Ir(H)_2(PNP^{iPr})CO$ instead of $Ir(H)_3(PNP^{iPr})$ resulted in no gas evolution, showing that the CO unit clearly has a detrimental effect to ability of the iridium-based PNP pincer complex to catalyse the MeOH reforming process. Moreover, a mechanism similar to that depicted in **Figures 3** and **4** were proposed.

Overall, aqueous-phase MeOH reforming by use of homogeneously catalysed AAD methods has witnessed great improvements during the last approximately 5 years. A variety of different metal based complexes has been demonstrated to catalyse the reaction with good activity and longevity. Nevertheless, there is still need for more in-depth studies to reveal the factors important for taking the methodology even further towards applicability.

4. Conclusion

Since the last decade, AAD by homogeneous catalysis has witnessed great improvements. Catalyst activity and stability has mainly been investigated with small molecule transformations,

such as methanol, ethanol and isopropanol. This is because with larger alcohol substrates, a more organic synthetic and preparative applicability is the main focus.

Moreover, particularly full methanol AAD corresponding to aqueous-phase methanol reforming currently enjoys much attention due to its possible use in renewable energy storage. Hence, since 2013, several interesting systems have been developed for this specific reaction, and many important insights have been disclosed. This sets the stage for taking this chemistry even further to the next level towards industrial applicability.

However, there is still lacking much research into the more subtle mechanism(s) and factors that are decisive for system efficiency and longevity. Furthermore, to date there has not been developed a reversible system for methanol AAD and CO_2 hydrogenation, which is imperative to achieve in order to reach a level ready for application. In addition, even more active systems are required. At best, these systems should work without any sacrificial additives to afford more economically viable reactions.

Acknowledgements

Author details

Martin Nielsen

Address all correspondence to: marnie@kemi.dtu.dk

Technical University of Denmark, Kongens Lyngby, Denmark

References

[1] Olah GA. Towards oil independence through renewable methanol chemistry. Angewandte Chemie, International Edition. 2013;**52**(1):104-107. DOI: 10.1002/anie.201204995

[2] Charman HBJ. Hydride transfer reactions catalysed by metal complexes. Journal of the Chemical Society B: Physical Organic. 1967. pp. 629-632. DOI: 10.1039/j29670000629

[3] Dobson A, Robinson SD. Catalytic dehydrogenation of primary and secondary alcohols by $Ru(OCOCF_3)_2(CO)(PPh_3)_2$. Journal of Organometallic Chemistry. 1975;**87**(3):C52-C53. DOI: 10.1016/S0022-328X(00)88159-0

[4] Dobson A, Robinson SD. Complexes of the platinum metals. 7. Homogeneous ruthenium and osmium catalysts for the dehydrogenation of primary and secondary alcohols. Inorganic Chemistry. 1977;**16**(1):137-142. DOI: 10.1021/ic50167a029

[5] Morton D, Cole-Hamilton DJ. Molecular hydrogen complexes in catalysis: Highly efficient hydrogen production from alcoholic substrates catalysed by ruthenium complexes. Journal of the Chemical Society, Chemical Communications. 1988;**2**(17):1154-1156. DOI: 10.1039/c39880001154

[6] Junge H, Beller M. Ruthenium-catalyzed generation of hydrogen from iso-propanol. Tetrahedron Letters. 2005;**46**(6):1031-1034. DOI: 10.1016/j.tetlet.2004.11.159

[7] Junge H, Loges B, Beller M. Novel improved ruthenium catalysts for the generation of hydrogen from alcohols. Chemical Communications. 2007;(5):522-524. DOI: 10.1039/B613785G

[8] Bertoli M, Choualeb A, Lough AJ, Moore B, Spasyuk D, Gusev DG. Osmium and ruthenium catalysts for dehydrogenation of alcohols. Organometallics. 2011;**30**(13):3479-3482. DOI: 10.1021/om200437n

[9] Nielsen M, Kammer A, Cozzula D, Junge H, Gladiali S, Beller M. Efficient hydrogen production from alcohols under mild reaction conditions. Angewandte Chemie, International Edition. 2011;**50**(41):9593-9597. DOI: 10.1002/anie.201104722

[10] Spasyuk D, Gusev DG. Acceptorless dehydrogenative coupling of ethanol and hydrogenation of esters and imines. Organometallics. 2012;**31**(15):5239-5242. DOI: 10.1021/om300670r

[11] Morton D, Cole-Hamilton DJ. Rapid thermal hydrogen production from alcohols catalysed by [Rh(2,2'-bipyridyl)$_2$]cl. Journal of the Chemical Society, Chemical Communications. 1987;**1**(4):248-249. DOI: 10.1039/C39870000248

[12] Morton D, Cole-Hamilton DJ, Utuk ID, Paneque-Sosa M, Lopez-Poveda M. Hydrogen production from ethanol catalysed by group 8 metal complexes. Journal of the Chemical Society, Dalton Transactions. 1989;(3):489-495. DOI: 10.1039/dt9890000489. http://pubs.rsc.org/en/content/articlelanding/1989/dt/dt9890000489#!divAbstract

[13] Nielsen M, Junge H, Kammer A, Beller M. Towards a green process for bulk-scale synthesis of ethyl acetate: Efficient acceptorless dehydrogenation of ethanol. Angewandte Chemie, International Edition. 2012;**51**(23):5711-5713. DOI: 10.1002/anie.201200625

[14] Sponholz P, Mellmann D, Cordes C, Alsabeh PG, Li B, Li Y, Nielsen M, Junge H, Dixneuf P, Beller M. Efficient and selective hydrogen generation from bioethanol using ruthenium pincer-type complexes. ChemSusChem. 2014;**7**(9):2419-2422. DOI: 10.1002/cssc.201402426

[15] Nielsen M, Alberico E, Baumann W, Drexler H-J, Junge H, Gladiali S, Beller M. Low-temperature aqueous-phase methanol dehydrogenation to hydrogen and carbon dioxide. Nature. 2013;**495**(7439):85-89. DOI: 10.1038/nature11891

[16] Bielinski EA, Förster M, Zhang Y, Bernskoetter WH, Hazari N, Holthausen MC. Base-free methanol dehydrogenation using a pincer-supported iron compound and Lewis acid co-catalyst. ACS Catalysis. 2015;**5**(4):2404-2415. DOI: 10.1021/acscatal.5b00137

[17] Alberico E, Lennox AJJ, Vogt LK, Jiao H, Baumann W, Drexler H-J, Nielsen M, Spannenberg A, Checinski MP, Junge H, Beller M. Unravelling the mechanism of basic aqueous methanol dehydrogenation catalyzed by Ru-PNP pincer complexes. Journal of the American Chemical Society. 2016;**138**(45):14890-14904. DOI: 10.1021/jacs.6b05692

[18] Friedrich A, Drees M, Schmedt auf der Günne J, Schneider S. Highly stereoselective proton/hydride exchange: Assistance of hydrogen bonding for the heterolytic splitting of H_2. Journal of the American Chemical Society. 2009;**131**(48):17552-17553. DOI: 10.1021/ja908644n

[19] Monney A, Barsch E, Sponholz P, Junge H, Ludwig R, Beller M. Base-free hydrogen generation from methanol using a bi-catalytic system. Chemical Communications. 2014;**50**(6):707-709. DOI: 10.1039/C3CC47306F

[20] Rodríguez-Lugo RE, Trincado M, Vogt M, Tewes F, Santiso-Quinones G, Grützmacher H. A homogeneous transition metal complex for clean hydrogen production from methanol–water mixtures. Nature Chemistry. 2013;**5**(4):342-347. DOI: 10.1038/nchem.1595

[21] Hu P, Diskin-Posner Y, Ben-David Y, Milstein D. Reusable homogeneous catalytic system for hydrogen production from methanol and water. ACS Catalysis. 2014;**4**(8):2649-2652. DOI: 10.1021/cs500937f

[22] Milstein D. Discovery of environmentally benign catalytic reactions of alcohols catalyzed by pyridine-based pincer Ru complexes, based on metal-ligand cooperation. Topics in Catalysis. 2010;**53**(13-14):915-923. DOI: 10.1007/s11244-010-9523-7

[23] Van de Watering F, Lutz M, Dzik W, de Bruin B, Reek JNH. Reactivity of a ruthenium-carbonyl complex in the methanol dehydrogenation reaction. ChemCatChem. 2016;**8**(17):2752-2756. DOI: 10.1002/cctc.201600709

[24] Alberico E, Sponholz P, Cordes C, Nielsen M, Drexler H-J, Baumann W, Junge H, Beller M. Selective hydrogen production from methanol with a defined iron pincer catalyst under mild conditions. Angewandte Chemie, International Edition. 2013;**52**(52):14162-14166. DOI: 10.1002/anie.201307224

[25] Andérez-Fernández M, Vogt LK, Fischer S, Zhou W, Jiao H, Garbe M, Elangovan S, Junge K, Junge H, Ludwig R, Beller M. A stable manganese pincer catalyst for the selective dehydrogenation of methanol. Angewandte Chemie, International Edition. 2017;**56**(2):559-562. DOI: 10.1002/anie.201610182

[26] Fujita K, Kawahara R, Aikawa T, Yamaguchi R. Hydrogen production from a methanol-water solution catalyzed by an anionic iridium complex bearing a functional bipyridonate ligand under weakly basic conditions. Angewandte Chemie, International Edition. 2015;**54**(31):9057-9060. DOI: 10.1002/anie.201502194

[27] Campos J, Sharninghausen LS, Manas MG, Crabtree RH. Methanol dehydrogenation by iridium N-heterocyclic carbene complexes. Inorganic Chemistry. 2015;**54**(11):5079-5084. DOI: 10.1021/ic502521c

[28] Prichatz C, Alberico E, Baumann W, Junge H, Beller M. Iridium-PNP pincer complexes for methanol dehydrogenation at low base concentration. ChemCatChem. 2017;**9**(11):1891-1896. DOI: 10.1002/cctc.201700015